Short Communication

Corrosion Inhibition of Aluminum in Hydrochloric acid Solution Using Ceria Doped Polyvinyl Chloride Nanofiber.

Soha Gaballah[1, 2,], Nader Shehata[1,3,4], Mohamed Shaaban[2], Shaaban Nosier[2], Ahmed Hefnawy[5], Aya Hamed[1, 4,] Effat Samir[1, 6]*

[1] Center of Smart Nanotechnology and Photonics (CSNP), SmartCI Research Center, Alexandria University, Alexandria 21544 Egypt.
[2] Department of Chemical Engineering, Faculty of Engineering, Alexandria University, Alexandria 21544 Egypt.
[3] USTAR Bioinnovations center, Utah State University, Logan 84341 Utah
[4] Department of Engineering Mathematics and Physics, Faculty of Engineering, Alexandria University, Alexandria 21544 Egypt.
[5] Department of Materials Science t, Institute of Graduate Studies and Research, Alexandria University, Alexandria, 21544 Egypt
[6] Department of Electrical Engineering, Faculty of Engineering, Alexandria University, Alexandria 21544, Egypt
[*]E-mail: soha_gaballah@mena.vt.edu

This aim of the percent work is to develop new, cost effective, high performance, lightweight polymer matrix composite nanofiber for corrosion resistance of aluminum in 0.1 M hydrochloric acid (0.1 M HCl) solution. Cerium oxide nanoparticles (ceria NPs) are embedded *in-situ* in *poly vinyl chloride (PVC)* solution, and then formed as nanofibers using electrospinning technique. The formed nanocomposite coating of PVC is successfully deposited on aluminum substrates; considering these substrates as metallic target in the electrospinning procedure. Measurements of corrosion for aluminum substrate before, and after coating with polymer nanofiber in 0.1 M HCl solution is performed using potentiodynamic polarization ,and electrochemical impedance spectroscopy techniques. Potentiodynamic polarization and electrochemical impedance results confirm that ceria NPS embedded in-situ within PVC NFS coatings protect the aluminum surface from being corroded through minimizing both of its corrosion rate, corrosion current and increasing the surfaces' polarization resistance. The morphologies of polymer nanofiber coatings are imaged using scanning electron microscopy (SEM), with detecting the optical characteristics of the synthesized nanocomposite to prove the existence of oxygen vacancies associated to tri-valent cerium ions via optical analysis such as direct band gap, and fluorescence measurements. These vacancies are considered physical adsorbers for radicals which consequently reduces the corrosion rate. Average mean diameter of ceria NPS was measured using   transmission electron microscopy (TEM).

1. INTRODUCTION

Aluminum is considered as the second most common metal in the Earth's crust. Aluminum, and its alloys are widely used in many applications as its low cost, high strength accomplished with low density and high thermal, and electrical conductivity .These advantages make it useful in different industries such as marine applications, aerospace, food packing, electronics, heat exchangers in petroleum industry, scrubbers and storage tanks [1-4]. Generally, Aluminum forms a protective invisible passive oxide film on its surface upon exposure to an aqueous solution ,but this oxide film does not offer sufficient protection against strong acidic, and alkaline solutions because of its solubility at these conditions, which increases the rate of corrosion .To decrease electrochemical corrosion of aluminum, some coaters such as synthetic polymers, organic, and inorganic compounds were used to isolate aluminum surface from corrosion medium by forming more resistant oxide film on metal surface [5-11]. Researchers found that rare earth elements such as cerium, lanthanum, neodymium, and yttrium might be an effective corrosion protection for aluminum because they control cathodic reaction. The maximum corrosion protection efficiency is improved with cerium because of the presence of Ce^{3+} [12-14]. In this research , the synthesized corrosion coat contains one of the promising lanthanide nanomaterials; cerium oxide (ceria) nanoparticles, which offer an advantage of tiny dimensions for being applicable of injecting them inside nanofiber; "*in-situ*" with polyvinyl chloride (PVC), nanofibers formed by the electrospinning technique. Electrospinning technique has been chosen as the fabrication technique for the formed nanocomposite. With a simple operation, ceria NPs could be embedded easily in the formed PVC nanofibers with the ability to scale- up to fabricate large volumes of the resulted nanocomposite [15]. It has been widely used in many applications, such as biomedical, gas sensors, electronics, and corrosion inhibition [16-21]. In this work, we report the synthesis of ceria NPs, and then embedded *in-situ* in polyvinyl chloride (PVC) nanofiber coating on aluminum substrates as a collector in the electrospinning process. The effect of polymeric coat on the corrosion behavior of aluminum in 0.1M HCl was examined using potentiodynamic polarization, and impedance spectroscopy. The surface of aluminum, and the Polymeric coated aluminum surface before, and after immersing in HCl were characterized by using scanning electron microscope (SEM). The synthesized nanocomposite has been optically characterized using absorbance spectroscopy, direct bandgap calculations, and fluorescence spectroscopy. These optical characterizations can give proof of the existence of oxygen vacancies inside the crystalline structure of ceria nanoparticles; which can adsorb the free radicals, and consequently reduce the rate of corrosion [22].

2. EXPERIMENTAL

2.1. Polymer and Nanoparticle Synthesis

During preparation of PVC solution, 12 wt. % polymer pellets is added to tetrahydrofuran solvent (anhydrous THF, ≥99.9%, Sigma Aldrich, St. Louis, MO, United States) ,and stirring overnight at 25°C. Ceria nanoparticles were synthesized using a chemical precipitation technique; similar to that

described by chen and chang, but with slight modifications in precursors and synthesis procedure [23, 24]. This technique has been chosen as it is simple, has easy procedure, and needs reasonable cost precursors. For the preparation of ceria NPs; firstly, 0.5 gm of cerium (III) chloride heptahydrate (99.9%, Sigma-Aldrich, St. Louis, MO, United States) is mixed with 40 ml of distilled water in an open container. After that, 1.6 ml of ammonia is added as a solvent, and the whole solution is magnetically stirred for 1.5 hrs, in water bath at temperature around 60 °C. Finally, the solution is allowed to cool at room temperature over the stirrer for 22.5 hrs. The long stirring period helps in fracturing of any nanorods produced into nanoparticles. The produced mixture; is then centrifuged, and washed twice with distilled water, and ethanol to get rid of any unreacted cerium, and ammonia. Ceria NPs with various weight percentages are added in-situ to the PVC solution. The electrospun mixture is stirred for 30 minutes before electro spinning process.

2.2. Electrospinning

As shown in Figure 1; the electrospinning Setup consists of four main parts; high voltage power supply (model CZE1000R, Spellman High Voltage Electronics Corporation, Hauppauge, New York, United States), a syringe pump (NE1000-Single Syringe Pump, New Era, and Farmingdale, New York, United States), and a collector. The syringe pump regulates the feed rate of polymer solution, and a 5 mL plastic syringe with an 18 gauge metallic needle is used to hold the polymer solution. The voltage power supply is connected to the needle, and the collector is grounded. The distance between the needle tip and the collector is fixed at 15cm. The voltage difference between the needle, and target is 20 kV. The flow rate of the polymer solution is fixed at 9 mL/h. The fibers were collected on target metals, and the running time of electrospinning process per sample is about 30 min.
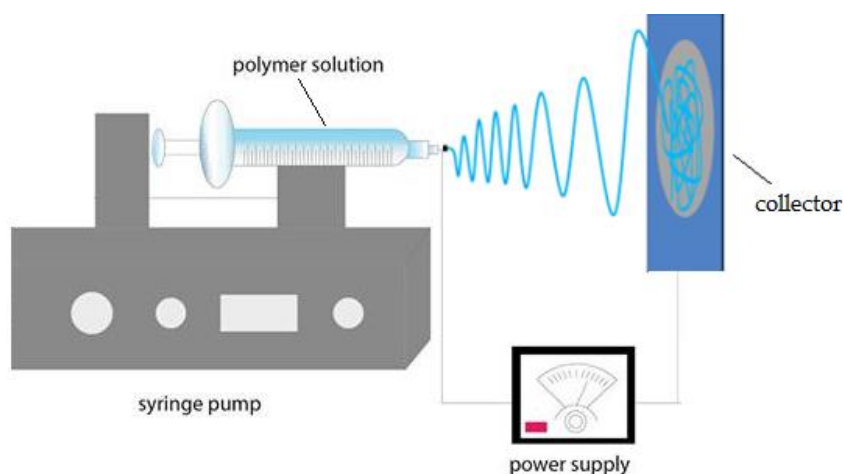

Figure 1. Schematic for electrospinning process

2.3. Corrosion test

The electrochemical measurements were performed in a three-electrode Pyrex cell with an overall volume of 100 cm$^{3.}$A platinum foil, and saturated calomel (SCE) was used as auxiliary, and

reference electrode, respectively. Measurements were carried out with a GAMRY G 750 instrument, and accompanying electrochemical software version 5.3. The polarization curves were obtained potentiodynamically between -0.25V, and 0.25 V relative to the open circuit potential with a scan rate of 1 mV s^{-1}. Electrochemical impedance spectroscopy experiments were conducted in a frequency range of 0.1 Hz - 100 kHz at open circuit potential by applying an alternating potential signal of 10 mV peak-to-peak. Echem analyst 5.5 software is used for graphing, and data fitting. All electrochemical experiments were carried out in aerated solutions under unstirred conditions at (30 ± 2) °C.

2.4. Nanocomposite characterization

PVC nanofibers with embedded ceria NPs; are optically characterized by measuring its optical absorbance, and fluorescence intensity curves. UV-Vis spectrophotometer T92 has been used to measure optical absorbance in a wavelength within range from 300 to 700nm. Corresponding NFs band gap can be determined from absorbance curves as explained in results and discussion section.

A setup of fluorescence spectroscopy is initiated by the authors for measuring the fluorescence intensity, as shown in Figure 2. Fluorescence setup consists of ultra-violet (UV) LED with 430nm excitation wavelength, Newport cornerstone 130 monochromator; which sweeps wavelength from 500 to 700nm and, measure corresponding frequency. Oriel photomultiplier tube (Newport PMT77340) is used as fluorescence intensity detector, and Newport 1918-R power meter is used to display PMT detection readings. For Fluorescence intensity measurement polymer NFs solid sample holder is positioned 45° between UV- LED and the input port of the monochromator. The output port of the monochromator was directly connected to PMT and consequently connected to the power meter.
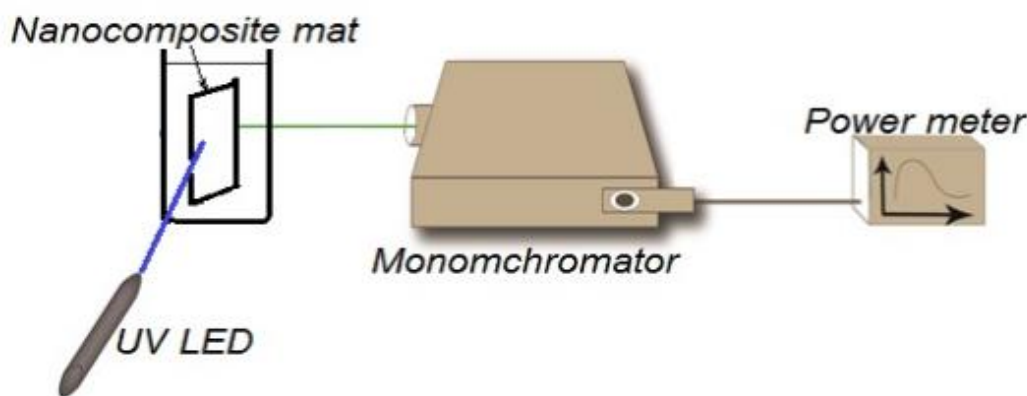

Figure 2. Fluorescence intensity hand-made spectroscopy setup

The polymer surface morphology nanofibers on aluminum surface before and after corrosion test were investigated by scanning electron microscopy (JSM-7100F). After sputter coating with gold, the fiber size distribution of randomly selected SEM micrographs was measured using the Image-J

software. The determination of mean size diameter of synthesized ceria NPs was observed by transmission electron microscopy (TEM) Panalytical's X'Pert PRO x-ray diffraction via Cu K_α radiation (λ=0.154 nm) is used to measure XRD analysis of the synthesized nanoparticles.

3. RESULTS AND DISCUSSION

3.1. Polarization Measurements

The polarization curves for the aluminum electrode coated with PVC NFs, and PVC NFs embedded in-situ ceria NPs with concentration (0.25,1,3,5 wt.%) in 0.1 M HCl at 25 ± 2°C, are shown in Figure3.Table 1 describes The values of corrosion current density (i_{corr}), corrosion potential (E_{corr}), anodic Tafel slope (β_a), cathodic Tafel slope (β_c), Corrosion Rate (C.R), and inhibition efficiency (IE%) obtained are illustrated in Table 1. Tafel fit routine provided by the Gamry Echem analyst software was used to calculate these values.It uses a non-linear chi-squared minimization to fit the data of the Stern-Geary equation. The inhibition efficiency was calculated from the following equation [25]:

$$IE(\%) = \frac{I - I^\circ}{I} \times 100 \tag{1}$$

where I and I° are the corrosion current before and after addition of corrosion coat, respectively.
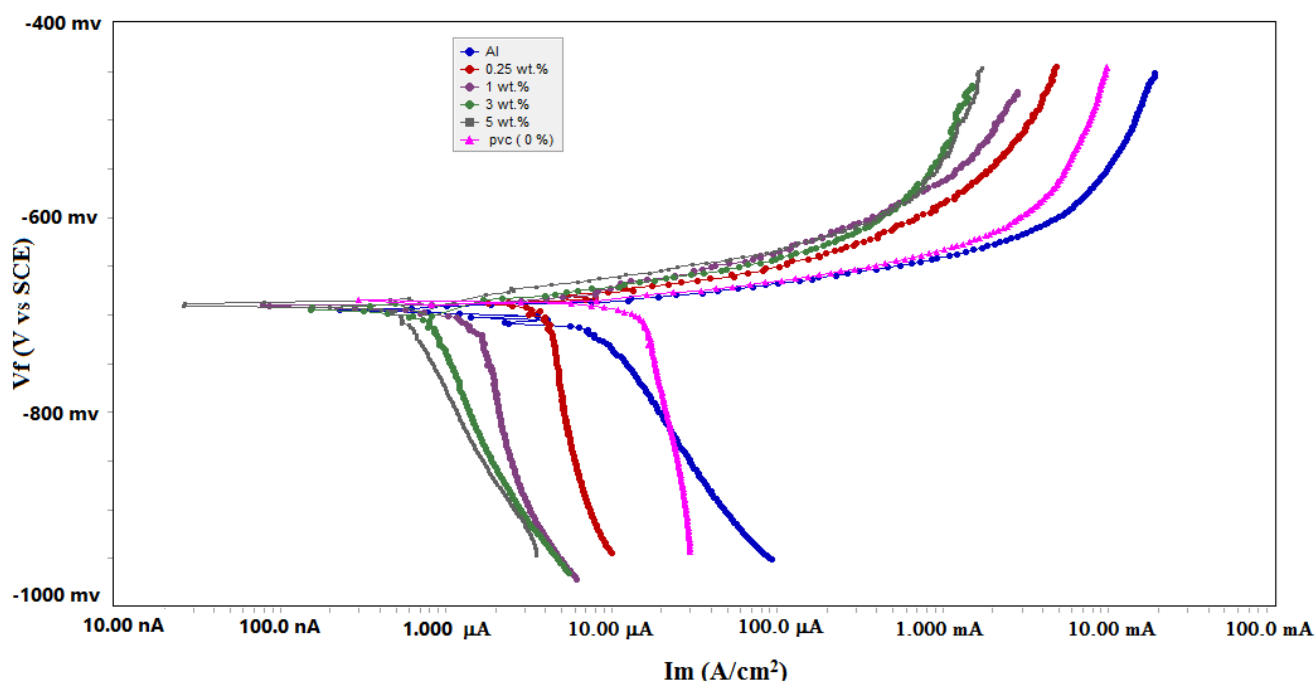

Figure 3. Tafel curves for electrochemical experiments of aluminium coated withPVC nanofiber ,with and without addition of ceria. in 0.1 M HCl m   Im (A/cm^2)

Table 1. Polarization parameters for aluminium in 0.1 M HCl with different coating materials at 25 ± 2°C.

Material	β_a (V.dec^{-1})	β_c (V.dec^{-1})	i_{corr} (μA.cm^{-1})	-Ecorr (mv)	C.R (mpy)	IE %
Al_substrate	30.20e^{-3}	163.4e^{-3}	4.96	695.0	6.389	0.00
PVC	40.20e^{-3}	1.000e^{15}	2.68	658.0	3.454	46
PVC-ceria 0.25 wt%	38.50e^{-3}	1.000e^{15}	2.38	683.0	2.045	52
PVC-ceria 1 wt%	38.90e^{-3}	1.000e^{15}	2.22	690.0	1.905	55.4
PVC-ceria 3 wt%	35.70e^{-3}	1.000e^{15}	1.37	694.0	1.760	72.4
PVC-ceria 5 wt%	32.30 e^{-3}	733.1e^{-3}	0.709	690.0	608.7e^{-3}	85.7

The inhibitor is considered either an anodic-type, or cathodic-type inhibitor when the displacement in E_{corr} is larger than 85 mV with respect to initial E_{corr} [26,27].In the present study;the maximum displacement was 37 mV, which indicates that the inhibitor is mixed-type. Adding PVC NFs, and PVC NFs embedded in-situ ceria NPs decreases the anodic dissolution of aluminum and retards the cathodic hydrogen evolution. Table 1 shows that the i_{corr} values is reduced in the presence of ceria NPs doped within PVC NFs and increasing of IE% . This result illustrates that the corrosion rate is decreased when coating the surface with PVC NFs embedded in-situ ceria NPs, and that the inhibition efficiency increases with increasing ceria concentration. The change in the values of the Tafel constants (βa and βc) when using polymeric coating indicates that the inhibitor controls both anodic and cathodic reactions compared without polymeric coating.
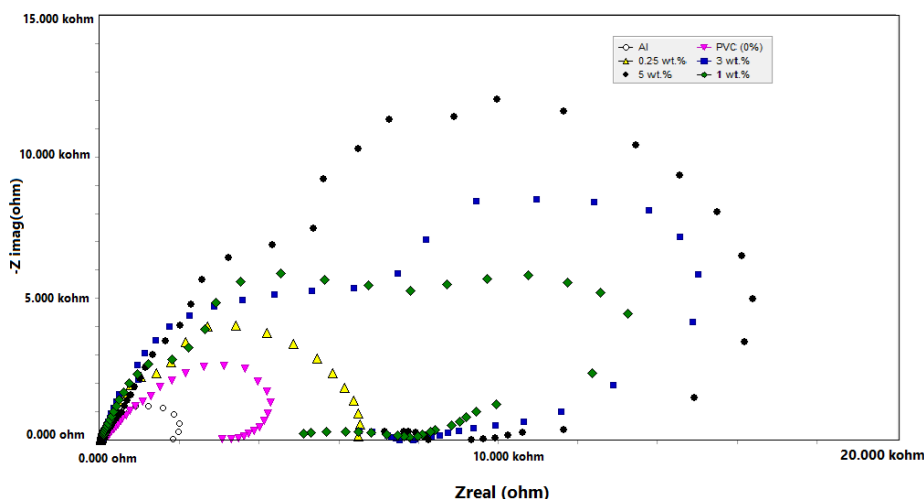
3.2. Impedance measurements

Figure 4. Nquist plot obtained for aluminium coated with PVC nanofiber ,before and after addition of ceria. in 0.1 M HCl
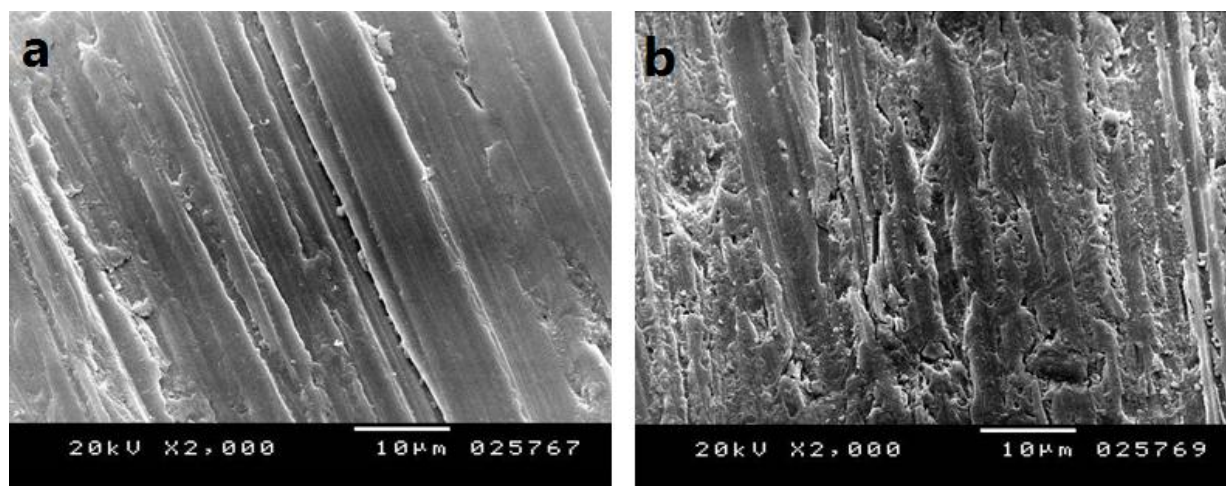
The electrochemical impedance spectroscopy curves for the aluminium electrode coated with PVC nanofiber and ceria doped insitu within PVC nanofiber in 0.1 M HCl at $25 \pm 2^{o}C$, are shown in Figure 4. As shown in figure there is an increase in the diameter of capacitive loop, with the increased concentration of ceria in PVC solution, which indicate that the corrosion resistance of aluminum increases gradually.This increasing in diameter is due to the high frequency of the capacitive loop which can accomplished with charging transfer reactions, and leads to formation of partial double layer capacitance on the alumium surface and that explains increasing of alumium resistance with increasing the diameter of capacitive loop.

3.3. Nanocomposite charcterization

The morphology, structure, and the distribution of the PVC NFs on the coated surfaces were investigated using scanning electron microscopy (SEM) analysis. Aluminum, blank sample, PVC NFs and PVC NFs embedded in-situ ceria NPs with concentration 3 wt% coated on aluminum surface were examined by SEM before and after immersing in 0.1 M HCl for 24 hrs. (C.f Figure 5).By comparing original reference sample before and after the corrosion test it could be observed that the sample has been corroded, and the grooves' contrast (depth) is not as visible as before the test as it is covered, and hidden by corrosion-produced compounds. This leads to the conclusion that hydrochloric solution has reached the whole surface including the bottom of the grooves [25].

SEM micrographs of PVC NFs, and PVC NFs embedded in-situ ceria NPs coated samples before and after the immersing in HCl clears that there is not a significant change in the surface appearance. The average mean diameter of PVC NFs is found to be about 620 nm, and mean diameter of PVC NFs embedded in-situ ceria NPs with concentration 3 wt% is found to be about 486 nm.

TEM for ceria NPs embedded in-situ with PVC nanofibers is shown in Figure 6. Ceria NPs is agglomerated inside the nanofibers. Both TEM image, and XRD pattern for ceria nanoparticles are shown in Figures 7 and 8, respectively. The average mean diameter of the nanoparticles is found to be about 6 nm.
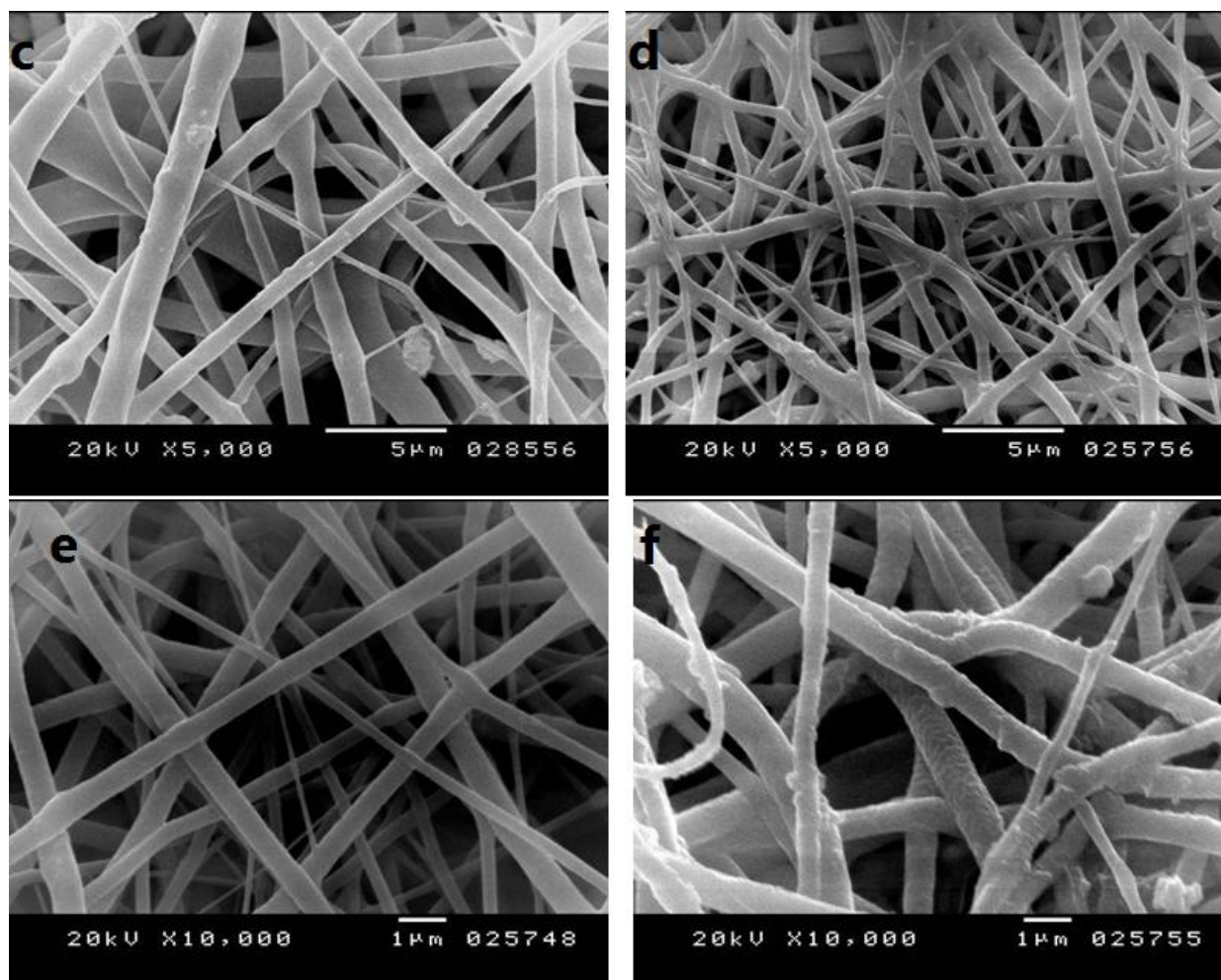
Figure 5. SEM images of the reference sample (Al) a) before and b) after immersion in 0.1 M HCl, PVC NFs coated on aluminum surface c) before and d) after immersion in 0.1 M HCl, PVC NFs embedded in-situ ceria NPs with concentration 3 wt% coated on aluminum surface e) before and f) after immersion in 0.1 M HCl.

Figure 6. TEM image of ceria NPs embedded in-situ with PVC nanofibers.

The crystalline structure of the doped nanoparticles is mainly composed of ceria NPs from the first diffraction peak of the most stable surface plane of ceria; (111) plane, the mean diameter is confirmed to be about 6 nm using Scherer's formula [28, 29].

$$d = \frac{0.9\lambda}{\beta \cos(\theta)} \tag{2}$$

Where d is the average particle size diameter, λ is the wavelength of X-ray, β is the full width half-maximum (FWHM) of the surface plane pattern, and θ is the diffraction angle.
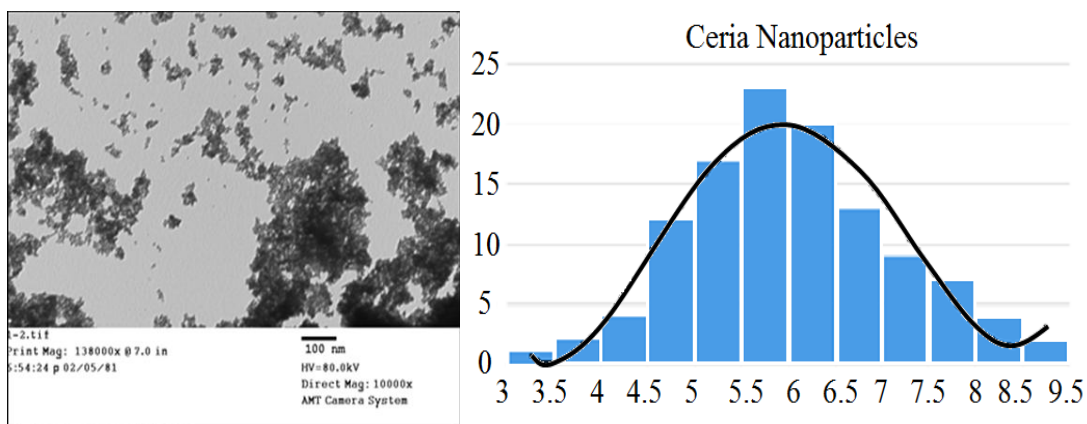

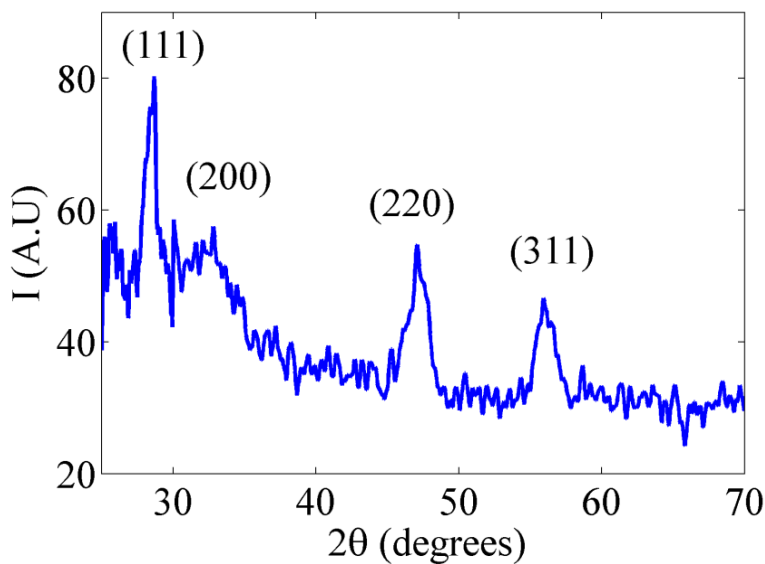**Figure 7.** TEM image of ceria NPs with mean grain size 6 nm.

Figure 8. XRD pattern of ceria NPs

3.4. Optical characterization of ceria NPs embedded in-situ with PVC nanofibers

The absorbance curves of ceria NPs doped within PVC NFs with concentrations; 1% and 5% are shown in Figure 9 a. The corresponding direct bandgap can be calculated from the absorbance dispersion curve through equation (3) [30].

$$\alpha(E) = A(E - E_g)^{1/2}$$

$$(3)$$

where α is the absorbance coefficient, A is a constant that depends on the effective masses of electrons, and holes in ceria NPs, E is the absorbed photon energy, and E_g is the allowed direct band gap. Figure 9.b shows the relation between $(\alpha E)^2$ versus E, and the intersection of the extrapolation of the linear part of $(\alpha E)^2$ curve with E (x-axis) is equal to allowed direct bandgap E_g that particular composition of ceria NPs with moderate concentration of tri-valent cerium ionization states with associated O-vacancies, which is within accepted range raised to 3 eV [31, 32]
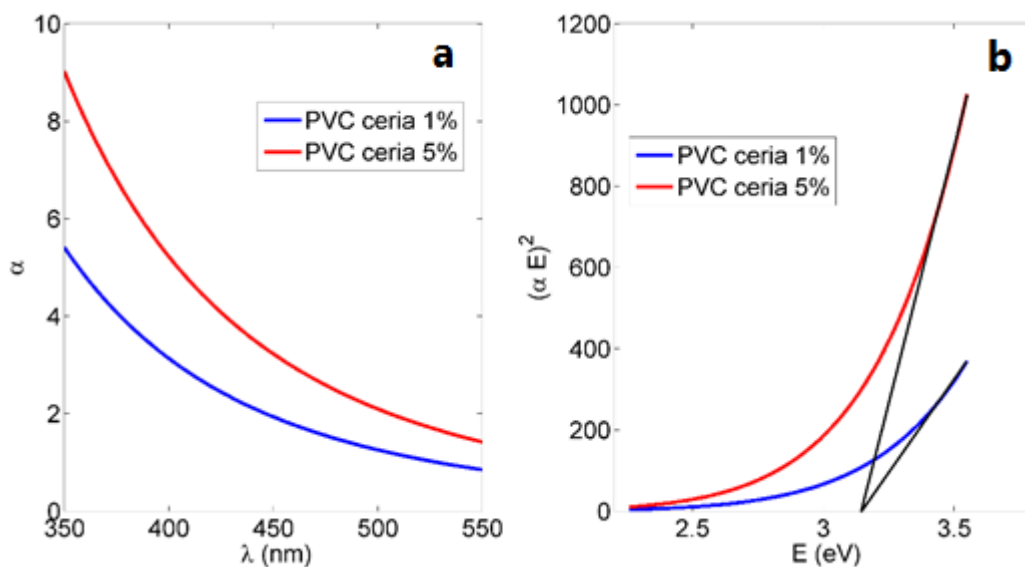

Figure 9. PVC NFs with in-situ embedded ceria NPs a) Absorbance curve b) Band gap curve
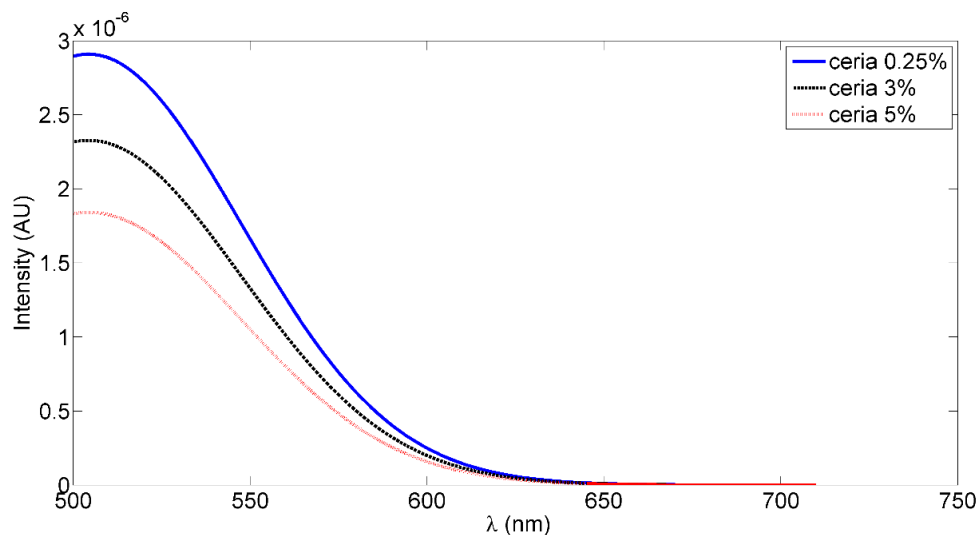

Figure 10. Fluorescence intensity PVC NFs with in-situ embedded different concentrations ceria NPs

Figure 10 shows the fluorescence intensity curves for the electrospun PVC NFs embedded in-situ with different ceria NPs concentrations for instance (0.25 wt. %, 3 wt. %, and 5 wt. %) were measured. Under near ultra violet UV excitation ~430nm; the corresponding resulted fluorescence

emission appears at wavelength approximately equals to 520nm. Since PVC NFs only are considered as a non-optical material, this optical fluorescence emission is as a result of the embedded ceria NPs [32].

4. CONCLUSIONS

The effect of PVC coatings on the corrosion behavior of aluminum 0.1 M HCl solutions was examined using cyclic potentiodynamic polarization (CPP) ,and electrochemical impedance spectroscopy (EIS) measurements. The surface morphologies of the formed nanofiber coatings before and after immersing in HCl for 24 hrs. are characterized using scanning electron microscopy (SEM) and the mean diameter of ceria NPs was examined using TEM analysis. The bandgap for ceria nanoparticles in all synthesized nanofibers was around 3.5 V; which indicates that it is still optically active [32]. Cyclic potentiodynamic polarization measurements show that coating the metal surface with PVC NFS reduces both corrosion currents, and corrosion rates, and increases the polarization resistances compared to uncoated surface.The results also illustrated as ceria concentration in PVC nanofiber increases, the corrosion rate decreases. EIS spectra confirmed that the ceria NPs doped PVC coated surfaces provided semicircles with bigger diameters; which indicates that these surfaces are more passivated. All measurements proved that coating the metal surface with PVC coating can protect to a great extent the aluminum against corrosion in 0.1 M HCl solution.

Abbreviations:

Ceria NPs: cerium oxide nanoparticles.
PVC: Poly-vinyl chloride.
SEM: Scanning Electron Microscope.
TEM: Transmission Electron Microscope.

References

1. J. Yue and Y. Cao, *Int. J. Electrochem. Sci.,* 10 (2015) 5222.
2. A. Fouda, M. Abdallah, I. Ahmed and M. Eissa, Arab. *J. Chem*, 5 (2012) 297.
3. G. Elewady, I. El-Said and A. Fouda, *Int. J. Electrochem. Sci.,* 3 (2008) 177.
4. J. E. Field and Trane, CORROSION OF ALUMINUM-FIN, COPPER-TUBE HEAT EXCHANGE COILS, Proceedings of the Thirteenth Symposium on Improving Building Systems in Hot and Humid Climates, Houston, TX, 2002,20 .
5. R. Hassan, I. Zaafarany, A.Gobouri and H. Takagi,*Int. J. Corros.*, 6 (2013) 0.
6. M.Es-saheb, A. Elzatahry, E. Sherif, A Alkaraki and E. kenawy, *Int. J. Electrochem. Sci.,* 7 (2012) 5962.
7. L. Molina-Ocampo, M .Valladares-Cisneros and J. Gonzalez-Rodriguez,*Int. J. Electrochem. Sci.,* 10 (2015) 383.
8. M. Arenas, M. Bethencourt, F.Botana, J. Damborenea and M. Marcos, *Corros. Sci, 43* (2001) 157.

9.   R. Hassan and I. Zaafarany, Mater. *Sci*, 6 (2013) 2436.
10. A. Fouda, K. Shalabi and N. Mohamed, *Int. J. Innov. Res. Sci*.., 3 (2014) 2319.
11. Q. Zhang and Y. Hua, *Mater. Chem. Phys*., 119 (2010) 57.
12. B. Hinton, D. Arnott and N. Ryan, *Met. Forum J*., 7 (1984) 211.
13. H. D. Johansen, C. Brett and A. Motheo, *Corros. Sci, 63* (2012) 342.
14. I. Kartsonakis, E. Koumoulos, A .Balaskas, G. Pappas, C. Charitidis and G. Kordas,   *Corros. Sci, 57* (2012) 56.
15. N. Shehata, E. Samir, S. Gaballah, A. Hamed and A. Elrasheedy, *Sensors,*16 (2016) 1371.
16. S. Agarwal, J. Wendorff and A. Greiner, *Polymers* (Basel, Switz.), 49 (2008) 5603.
17. S. Sell, P. Wolfe , K. Garg , J. McCool , I. A. Rodriguez and G. Bowlin, *Polymers* (Basel, Switz.) 2 (2010) 522.
18. B. Ding, M. Wang, J. Yu, G. Sun, *Sensors*, 9 (2009)1609.
19. A. Luzio, E. V. Canesi, C. Bertarelli and M. Caironi, *Mater. Sci.,* 7 (2014) 906.
20. M. Es-saheb, E. Sherif, A. El-Zatahry, M. El Rayes and K. A. Khalil, *Int. J. Electrochem. Sci.,* 7 (2012) 10442.
21. E. M. Sherif , M. Es-saheb, A. El-Zatahry , E. kenawy and A. Alkaraki, *Int. J. Electrochem. Sci.,* 7 (2012) 6154.
22. N, Shehata, E. Samir and S. Gaballah, *Sens. Actuators, B*, 231 (2016) 341.
23. N. Shehata, K. Meehan, M. Hudait, N. Jain and S. Gaballah, *Nanomaterials*, 5 (2014) 1.
24. H. Chen and H. Chang *Colloids Surf. A*, 242(2014) 61.
25. A. Toloei, V. Stoilov and D. Northwood, *Mater. Charact.* , 77 (2013) 193.
26. A. Al-Amiery, A. Kadhum, A. Mohamad, A. Musa and C. Li, *Mater. Sci.,* 6 (2013) 5466.
27. W.li, Q.He, S. Zhang and C. Pei, *J. Appl. Electrochem*., 38 (2008) 289.
28. S. Deshpande, S. Patil, S. Kuchibhatla and S. Seal, *Appl. Phys. Lett*., 87 (2015) 1.
29. B. D. Cullity and S. R. Stock, Elements of x-ray diffraction, Addison-Wesley Publisher (2001) Boston, United States
30. J. I. Pankove, Optical processes in semiconductors, Dover Publications, (1971) United States, New York.
31. E. Goharshadi, S. Samiee and   P. Nancarrow, *Adv. Colloid Interface Sci*., 356 (2011) 474.
32. N. Shehata, K Meehan, M. Hudait and M. Jai, *J. Nanopart.,* 14 (2012) 1173.